

# pQCT provides better prediction of canine femur breaking load than does DXA

K.C. Moio<sup>1,3</sup>, G. Podolskaya<sup>2</sup>, B. Barnhart<sup>3</sup>, A. Berzins<sup>3</sup>, D.R. Sumner<sup>1,3</sup>

<sup>1</sup>Department of Anatomy and Cell Biology, Rush Medical College, Chicago, IL, <sup>2</sup>Scholl School of Podiatric Medicine, Chicago, IL, <sup>3</sup>Department of Orthopedic Surgery, Rush Medical College, Chicago, IL, USA

## Abstract

Our study was designed to examine the validity of dual energy X-ray absorptiometry (DXA) and peripheral quantitative computed tomography (pQCT) measurements as predictors of whole bone breaking strength in beagle femora. DXA was used to determine the bone mineral content, bone area, and "areal" bone mineral density. pQCT was used to determine the cross-sectional moments of inertia, volumetric densities of the bone, and to calculate bone strength indices based on bone geometry and density. A three-point bending mechanical test was used to determine maximal load. Three variables from the pQCT data set explained 88% of the variance in maximal load, with the volumetric bone mineral density explaining 32% of the variance. The addition of the volumetric cortical density increased the adjusted  $r^2$  to 0.601 ( $p=0.001$ ) and the addition of an index created by multiplying volumetric cortical bone density by the maximum cross-sectional moment of inertia made further significant ( $p<0.001$ ) improvements to an adjusted  $r^2$  of 0.877. In comparison, when only the DXA variables were considered in a multiple regression model, areal bone mineral density was the only variable entered and explained only 51% ( $p<0.001$ ) of the variance in maximal load. These results suggest that pQCT can better predict maximal load in whole beagle femora since pQCT provides information on the bone's architecture in addition to its volumetric density.

**Keywords:** Bone Mechanics, Bone Density, Dual Energy X-ray Absorptiometry (DXA), pQCT, Femur

## Introduction

Non-invasive bone densitometry is commonly used in the clinical setting to assess bone density and the efficacy of treatment for osteoporosis. Dual energy X-ray absorptiometry (DXA) or peripheral quantitative computed tomography (pQCT) have been used to make such determinations. These techniques differ in their measurement parameters, the types of data collected, and their mode of calculating bone density. Since these data, in conjunction with other factors, are often used to assess fracture risk in patients, there is debate about which method provides the best index of bone strength. The experiment reported here compares the ability of DXA and pQCT to predict whole bone breaking strength of adult beagle femora.

The standard in clinical bone density analysis is DXA.

This technique offers information on the "areal density" but does not measure volumetric density and provides only limited information on the bone's architecture. DXA provides very precise measurements of bone mineral content (BMC) in grams, the area of the scanned region in  $\text{cm}^2$ , and "areal" bone mineral density (aBMD=BMC/area) in  $\text{g}/\text{cm}^2$ . Despite a relative lack of architectural information, many studies<sup>1-5</sup> have used aBMD and/or BMC to predict the probability of fracture (fracture risk) in individuals.

Information from pQCT includes volumetric bone densities, total (vTotBMD) and cortical (vCtBMD), and a set of geometric variables that characterize the architecture of the bone. The geometric variables that have offered a substantial amount of information regarding long bone strength are the cross-sectional moments of inertia (CSMI)<sup>6</sup>. The cross-sectional moment of inertia is a measure of the distribution of material around a given axis<sup>7</sup>. It is used to calculate the bone strength index (BSI) which is determined by multiplying CSMI by the volumetric cortical bone density<sup>8</sup>. In some previous studies, geometric variables individually or in conjunction with bone mineral density have furnished significant relationships with breaking strength<sup>9-17</sup>.

Corresponding author: Kirsten C. Moio, Department of Orthopedic Surgery, 1653 W. Congress Parkway, Suite 1471 Jelke, Chicago, IL 60612, USA  
E-mail: kirsten\_moio@rush.edu

Accepted 17 July 2003

	Minimum	Maximum	Mean	Standard deviation	COV (%)	Max to Min ratio
<b>Maximal load (N)</b>	1312	2975	2074	544	26	2.3
<b>pQCT variables</b>						
Iy (mm <sup>4</sup> )	465	1286	805	201	25	2.8
Ix (mm <sup>4</sup> )	353	1139	669	176	26	3.2
I <sub>max</sub> (mm <sup>4</sup> )	535	1346	848	205	24	2.5
I <sub>min</sub> (mm <sup>4</sup> )	348	1078	625	167	27	3.1
I <sub>max</sub> :I <sub>min</sub>	1.2	1.5	1.4	0.1	7	1.3
I <sub>p</sub> (mm <sup>4</sup> )	883	2424	1474	370	25	2.7
θ (degrees)	-22	33	9	14	156	N/A
TA (mm <sup>2</sup> )	79	139	108	15	14	1.8
CA (mm <sup>2</sup> )	49	82	64	8	13	1.7
vTotBMD (mg/cm <sup>3</sup> )	635	954	805	82	10	1.5
vCtBMD (mg/cm <sup>3</sup> )	1250	1356	1311	29	2	1.1
BSII <sub>max</sub>	695,964	1,746,840	1,106,655	269,045	24	2.5
BSII <sub>min</sub>	469,929	1,397,881	816,553	216,280	26	3.0
BSII <sub>x</sub>	476,765	1,476,828	874,969	229,955	26	3.1
BSII <sub>y</sub>	587,703	1,667,894	1,048,239	260,596	25	2.8
BSII <sub>p</sub>	1,191,090	3,144,724	1,923,208	482,210	25	2.6
<b>DXA variables</b>						
aBMD (g/cm <sup>2</sup> )	0.530	0.750	0.657	0.054	8	1.4
BMC (g)	1.888	3.350	2.675	0.319	12	1.8
Area (cm <sup>2</sup> )	3.560	4.636	4.063	0.274	7	1.3

Values for maximal load, pQCT, and DXA variables.

**Table 1.** Cross-sectional moments of inertia about anatomical axes (Ix, Iy), maximum and minimum moments of inertia (I<sub>max</sub>, I<sub>min</sub>), their ratios (I<sub>max</sub>:I<sub>min</sub>), polar moment of inertia (I<sub>p</sub>), orientation of the principle axes with respect to the anatomical axes (θ), total area (TA), cortical area (CA), volumetric total density (vTotBMD), volumetric cortical density (vCtBMD), bone strength indices (BSI) based on cortical density and the area and polar moments of inertia (BSII<sub>x</sub>, BSII<sub>y</sub>, BSII<sub>max</sub>, BSII<sub>min</sub>, BSII<sub>p</sub>), bone mineral density (aBMD), bone mineral content (BMC), and bone area.

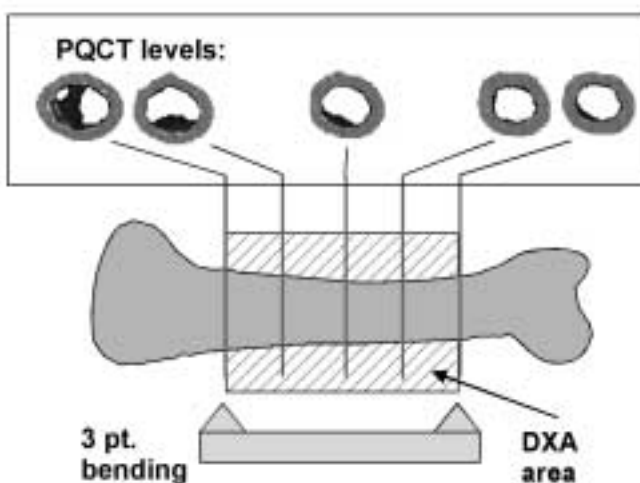


**Figure 1.** Sites of DXA scan, 5 pQCT cross-sectional scans, and the 3-point bending mechanical test.

From an engineering perspective, the prediction of whole bone strength depends on the bone's tissue-level (apparent) mechanical properties, their distribution in space (geometry), and the loading conditions<sup>18</sup>. The tissue-level mechanical properties are strongly dependent upon density. In many situations the geometry of the bony elements is just as important when gauging the whole bone breaking strength<sup>19</sup>. Standard bone densitometry (DXA) does not explicitly evaluate either the bone geometry or the apparent density. Nevertheless, DXA measurements are known to correlate with whole bone strength. Therefore, the aim of our study was to determine if the breaking load of whole beagle femora could be better predicted using DXA or pQCT measures of bone density and geometry.

## Materials and methods

A group of twenty-three fresh frozen beagle femora (11 female, 12 male; age range 1.16-13.30 yr; weight range 7.3-

pQCT and DXA variables	Component			% of Variance	Cumulative %
	1	2	3		
BSII <sub>max</sub>	.990			70.5	70.5
Imax (mm <sup>4</sup> )	.989				
BSII <sub>p</sub>	.988				
Ip (mm <sup>4</sup> )	.982				
BSII <sub>y</sub>	.974				
TA (mm <sup>2</sup> )	.973				
BSII <sub>min</sub>	.971				
BSII <sub>x</sub>	.968				
Iy (mm <sup>4</sup> )	.965				
Ix (mm <sup>4</sup> )	.965				
Imin (mm <sup>4</sup> )	.959				
DXA Area (cm <sup>2</sup> )	.953				
CA (mm <sup>2</sup> )	.812				
BMC (g)	.790				
θ (degrees)	.689				
vTotBMD (mg/cm <sup>3</sup> )		.925		13.9	84.4
aBMD (g/cm <sup>2</sup> )		.896			
vCtBMD (mg/cm <sup>3</sup> )			.880	9.6	94.0
Imax:Imin			.866		

**Table 2.** Results of the factor analysis (principal component analysis with varimax rotation) with pQCT and DXA variables. Shaded variables indicate variables with the highest loading used in the multiple regression analysis reported in Table 4.

17.7 kg) were collected for DXA, pQCT, and mechanical testing. The bones came from animals in IACUC approved studies, and had not been treated with any substances that could influence the bones. All femora were from left extremities. The femora were scanned with a dual energy X-ray absorptiometer (model DPX-L, Lunar Radiation) using small animal software (Version 1.0d) in the appendicular scan mode. During scanning the femur was placed on a 2.5 cm thick piece of Plexiglas to simulate soft tissues with the anterior surface facing up and the proximal end toward the head of the table. Measurements of BMC, bone area, and aBMD were obtained by analyzing a 35 mm long section from the shaft of the bone centered on the mid-femur (Figure 1). Edge detection of the femur during the DXA analysis was manually determined. Coefficients of variation for five measurements obtained for BMD, BMC, and area of the same femur after repositioning were 2.6%, 1.2%, and 2.1%, respectively.

pQCT scans of the femora were made on a XCT 960 pQCT X-ray bone densitometer (Norland Stratec) using small animal software (Version 5.10). Five cross-sectional scans (2 distally, 1 at the midshaft, and 2 proximally) were performed within the same 35 mm length of femur as the DXA scans (Figure 1). The two proximal scans were located 8.8 mm apart as were the two distal scans and the intermediate scan was centered on the mid-femur. Analyses of these

scans produced measurements of volumetric total density (vTotBMD), total area (TA), volumetric cortical density (vCtBMD), cortical area (CA), cross-sectional moments of inertia about anatomical axes (Ix, Iy), the maximum and minimum moments of inertia (Imax, Imin), the polar moment of inertia (Ip), the orientation of the principle axes with respect to the anatomical axes (θ), and strength indices based on vCtBMD multiplied by each cross-sectional moment of inertia (BSII<sub>x</sub>, BSII<sub>y</sub>, BSII<sub>max</sub>, BSII<sub>min</sub>, BSII<sub>p</sub>). Relatively high Iy (or BSII<sub>y</sub>) values compared to Ix (or BSII<sub>x</sub>) imply relatively greater resistance to bending in the medial-lateral direction than in the anterior-posterior direction. For the analysis procedure the contour mode was set at 2 and the peel mode was set at 5. The values for the 5 scans were averaged. Coefficients of variation obtained for vCtBMD and CA of the same femur after repositioning five times were 0.91% and 1.18%, respectively.

The femora then underwent a three-point bending mechanical test on a material testing machine (Instron, Model 1321) to determine maximal load (N) following the method of Martin et al.<sup>20</sup>. The femur was placed with the anterior surface facing down on a stand providing two points of support 35 mm apart. A posterior to anterior load was applied to the midshaft of the femur at 5 mm/min until failure. This loading site was the same location as the midshaft cross-sectional pQCT scan.

	Max load	BSII max	Imax	BSIIp	Ip	BSIIy	BSII min	Iy	TA	BSIIx	Imin	Ix	DXA area	CA	BMC	Θ	vTot BMD	a BMD	vCt BMD
BSII max	.13																		
Imax	.16	.99**																	
BSIIp	.16	.99**	.99**																
Ip	.19*	.97**	.99**	.99**															
BSIIv	.22*	.97**	.98**	.97**	.966**														
BSII min	.20*	.95**	.96**	.98**	.99**	.94**													
Iy	.25*	.95**	.97**	.96**	.97**	.99**	.94**												
TA	.05	.89**	.91**	.91**	.92**	.85**	.90**	.85**											
BSIIx	.10	.94**	.94**	.96**	.95**	.87**	.96**	.85**	.92**										
Imin	.22*	.92**	.95**	.96**	.98**	.93**	.99**	.94**	.90**	.94**									
Ix	.12	.93**	.94**	.96**	.96**	.87**	.97**	.87**	.93**	.99**	.96**								
DXA area	.10	.86**	.88**	.86**	.87**	.89**	.83**	.90**	.87**	.76**	.83**	.77**							
CA	.59**	.74**	.77**	.77**	.78**	.82**	.77**	.84**	.53**	.65**	.78**	.67**	.62**						
BMC	.45**	.72**	.70**	.71**	.68**	.77**	.68**	.75**	.46**	.59**	.65**	.57**	.58**	.90**					
Θ	.18*	.48**	.47**	.46**	.44**	.56**	.42**	.54**	.32**	.33**	.40**	.31**	.49**	.51**	.57**				
vTot BMD	.35**	.03 (-)	.03 (-)	.03 (-)	.04(-)	.01 (-)	.03 (-)	.01 (-)	.19 (-)	.07 (-)	.04 (-)	.08 (-)	.09(-)	.06	.09	.02			
aBMD	.54**	.22*	.20*	.21*	.19*	.26*	.20*	.23*	.05	.15	.18	.14	.09	.55**	.71**	.28**	.50**		
vCt BMD	.12(-)	<.01	.01(-)	<.01(-)	.02 (-)	<0.1(-)	.01(-)	.02(-)	.02(-)	<.01(-)	.04(-)	.01	.02(-)	.02(-)	.02	.02	.08	.09	
Imax: Imin	.22*(-)	.04 (-)	.06 (-)	.09(-)	.12(-)	.06 (-)	.17(-)	.08(-)	.12(-)	.12(-)	.20(-)	.16(-)	.05(-)	.10(-)	.03(-)	<.01	.03	<.01	.35**

\*p<0.05  
\*\*p<0.01

A minus sign within parentheses (-) indicates a negative correlation

**Table 3.** Univariate correlations (r2) for pQCT and DXA variables.

Statistical analyses of the data were performed using SPSS for Windows (Version 8.0). First, a factor analysis technique (principal component analysis with varimax rotation) was performed to group the pQCT and DXA variables (independent variables) into components based on their interrelationships. Based on the results from the factor analysis, the variables with the highest loading from each component were then used in a forward stepwise multiple regression analysis to determine which pQCT and DXA variables explained most of the variance in maximal load. The criteria for entering a variable was p=0.05 and for eliminating a variable after having been entered was p=0.1.

**Results**

The mean load at failure was 2,074 N, with a 2.3-fold variation from the weakest to the strongest bone (Table 1). The variation in the CSMIs tended to be about 3-fold whereas the variation in vCtBMD was less than 1.1-fold. The variation in vTotBMD and the DXA variables was about 1.5-fold.

In the factor analysis the pQCT and DXA variables were grouped into three components (Table 2) with all nineteen

variables contributing to the model explaining 94% of the variance. Component 1 contained most of the geometric pQCT variables and bone strength indices and contributed 70.5% of the variance. The areal and volumetric densities were placed in component 2 or 3, explaining 13.9% and 9.6% of the variance, respectively. For each of the three components, the variable with the highest loading was a pQCT variable (range 0.99-0.88) and specifically were BSIImax, vTotBMD, and vCtBMD. These three pQCT variables were then used in the forward stepwise multiple regression analysis. As expected, the variables that were grouped together to comprise each component were significantly correlated with the other variables within the component (Table 3).

In the multiple regression analysis (Table 4) all three pQCT variables entered the model and explained a total of 88% of the variance in maximal load. The regression analysis revealed that vTotBMD was the single best variable at predicting maximal load with an adjusted r<sup>2</sup> of 0.32 (p=0.003). The addition of vCtBMD increased the adjusted r<sup>2</sup> to 0.601 (p=0.001) and the addition of BSIImax made further significant (p<0.001) improvements to an adjusted r<sup>2</sup> of 0.877. Taken individually, each of these variables explained about 30% of the variance in maximal load.

Variables in:	Adjusted $r^2$	$\Delta$ Adjusted $r^2$	Significance
vTotBMD	0.32	0.32	0.003
vCtBMD	0.60	0.28	0.001
BSIImax	0.88	0.28	<0.001
Results of the forward stepwise multiple regression analysis with maximal load as the dependent variable.			

**Table 4.** Values are reported as adjusted  $r^2$ ,  $p_{in}=0.05$ ,  $p_{out}=0.1$ . Variables entered into the equation were BSIImax, vTotBMD, and vCtBMD.

As a comparison, when all pQCT and DXA variables were entered into a forward stepwise multiple regression analysis, results indicated that four pQCT variables entered the model explaining 96.6% of the variance in maximal load. The single best variable at predicting maximal load was CA (adj.  $r^2=0.572$ ,  $p<0.001$ ). The addition of BSIImax increased the adjusted  $r^2$  to 0.929 ( $p<0.001$ ) and the addition of Imax:Imin and BSIIp made further slight, but significant ( $p=0.015$ ), improvements. Interestingly, when only the DXA variables (aBMD, BMC, area) were considered in a multiple regression model, aBMD was the only variable entered and explained only 51% ( $p<0.001$ ) of the variance in maximal load.

## Discussion

The central finding of the present study was that pQCT provided better information than DXA for predicting the whole bone breaking strength of beagle femora. When only pQCT variables were considered, the multiple regression analysis showed that a combination of geometric and densitometric information explained 88% of the variance in maximal load.

In agreement with our finding that geometric variables make a contribution to predicting bone strength, Ferretti and co-workers<sup>8</sup> reported a significant correlation between BSI (CSMI x vCtBMD) and fracture load in rat femurs ( $r=0.94$ ), and Jamsa and co-workers<sup>21</sup> found that the breaking force of mouse femurs was best explained by CSMI and vCtBMD together ( $r=0.92$ ). Similarly, this relationship between geometric properties from QCT and their ability to predict fracture load in cadaver whole bone femora has been reported at the femoral neck ( $r=0.81$ )<sup>22</sup>, and at the mid-shaft ( $r=0.73$ )<sup>23</sup>.

It is interesting to note that there was very little variation in cortical bone density in this sample, whereas the variability in the total bone density from pQCT (vTotBMD) was about the same as the variability in aBMD from DXA. This implies that the source of variation in aBMD and vTotBMD was variation in cortical area rather than variation in cortical density. In other words, bones with thicker cortices appeared

denser when quantitated as aBMD or vTotBMD, but in actuality, the bone at a tissue level had a relatively constant density.

The main limitation of our study was the use of beagles that had a small range of body weights and bone mineral density measures (maximum 3-fold variation). In addition, the animals spanned a wide age range quite possibly providing a wide range of material properties. Unfortunately, the bone material properties and their microstructural determinants cannot be measured absorptiometrically. Thus, one must generalize with caution. However, previous validation of pQCT has come from small animal models and this work extends these observations to larger species.

## Conclusion

Our findings of the importance of bone geometry and density to whole bone strength are consistent with other studies, as cited above. Our results indicate that beagle femur whole bone strength can be better predicted by pQCT than DXA since pQCT provides information on the bone's architecture in addition to its density.

### Acknowledgments

NIH Grants AR16485 and AR42862.

*We would also like to acknowledge our co-author, Dr. Aivars Berzins, whose young life was ended too soon. He was a valuable member of our department and integral to the success of this paper. We would like to dedicate this paper in his memory.*

## References

1. Cummings SR, Black DM, Nevitt MC, Browner W, Cauley J, Ensrud K, Genant HK, Palermo L, Scott J, Vogt TM. Bone density at various sites for prediction of hip fractures. *Lancet* 1993; 341:72-75.
2. De Laet CE, Van Hout BA, Burger H, Weel AE, Hofman A, Pols HA. Hip fracture prediction in elder-

- ly men and women: validation in the Rotterdam study. *J Bone Miner Res* 1998; 13:1587-1593.
3. Doboef F, Hans D, Schott AM, Kotzki PO, Favier F, Marcelli C, Meunier PJ, Delmas PD. Different morphometric and densitometric parameters predict cervical and trochanteric hip fracture: The EPIDOS study. *J Bone Miner Res* 1997; 12:1895-1902.
  4. Lunt M, Felsenberg D, Reeve J, Benevolenskaya L, Cannata J, Dequeker J, Dodenhof C, Falch JA, Masaryk P, Pols HA, Poor G, Reid DM, Scheidt-Nave C, Weber K, Varlow J, Kanis JA, O'Neill TW, Silman AJ. Bone density variation and its effects on risk of vertebral deformity in men and women studied in thirteen European centers: the EVOS study. *J Bone Miner Res* 1997; 12:1883-1894.
  5. Melton LJ III, Atkinson EJ, O'Fallon WM, Wahner HW, Riggs BL. Long-term fracture prediction by bone mineral assessed at different skeletal sites. *J Bone Miner Res* 1993; 8:1227-1233.
  6. Milgrom C, Giladi M, Simkin A, Rand N, Kedem R, Kashtan H, Stein M, Gomori M. The area moment of inertia of the tibia: a risk factor for stress fractures. *J Biomech* 1989; 22:1243-1248.
  7. Turner CH, Burr DB. Basic biomechanical measurements of bone: a tutorial. *Bone* 1993; 14:595-608.
  8. Ferretti JL, Capozza RF, Zanchetta JR. Mechanical validation of a tomographic (pQCT) index for noninvasive estimation of rat femur bending strength. *Bone* 1996; 18:97-102.
  9. Brodt MD, Ellis CB, Silva MJ. Growing C57B1/6 mice increase whole bone mechanical properties by increasing geometric and material properties. *J Bone Miner Res* 1999; 14:2159-2166.
  10. Cheng XG, Lowet G, Boonen S, Nicholson PHF, Brys P, Nijs J, Dequeker J. Assessment of the strength of proximal femur *in vitro*: relationship to femoral bone mineral density and femoral geometry. *Bone* 1997; 20:213-218.
  11. Esses SI, Lotz JC, Hayes WC. Biomechanical properties of the proximal femur determined *in vitro* by single-energy quantitative computed tomography. *J Bone Miner Res* 1989; 4:715-722.
  12. Ferretti JL, Capozza RF, Mondelo N, Montuori E, Zanchetta JR. Determination of femur structural properties by geometric and material variables as a function of body weight in rats. Evidence of a sexual dimorphism. *Bone* 1993; 14:265-270.
  13. Ferretti JL, Capozza RF, Mondelo N, Zanchetta JR. Interrelationships between densitometric, geometric, and mechanical properties of rat femora: inferences concerning mechanical regulation of bone remodeling. *J Bone Miner Res* 1993; 8:1389-1396.
  14. Jamsa T, Tuukkanen J, Jalovaara P. Femoral neck strength of mouse in two loading configurations: method evaluation and fracture characteristics. *J Biomech* 1998; 31:723-729.
  15. Jurist JM, Foltz AS. Human ulnar bending stiffness, mineral content, geometry, and strength. *J Biomech* 1977; 10:455-459.
  16. Martens M, Van Audekercke R, De Meester P, Mulier JC. Mechanical behaviour of femoral bones in bending loading. *J Biomech* 1986; 19:443-454.
  17. Wilhelm G, Felsenberg D, Bogusch G, Willnecker J, Thaten J, Gummert P. Biomechanical examinations for validation of the bone strength strain index SSI, calculated by peripheral quantitative computed tomography. In: Lyritis GP (ed) *Musculoskeletal Interactions*, Vol. 2. Hylonome Editions, Athens, Greece; 1999:105-110.
  18. Hayes WC, Piazza SJ, Zysset PK. Biomechanics of fracture risk prediction of the hip and spine by quantitative computed tomography. *Radiol Clin North Am* 1991; 29:1-18.
  19. Seeman E. An exercise in geometry. *J Bone Miner Res* 2002; 17:373-380.
  20. Martin RB, Butcher RL, Sherwood LL, Buckendahl P, Boyd RD, Farris D, Sharkey N, Dannucci G. Effects of ovariectomy in beagle dogs. *Bone* 1987; 8:23-31.
  21. Jamsa T, Jalovaara P, Peng Z, Vaananen HK, Tuukkanen J. Comparison of three-point bending test and peripheral quantitative computed tomography analysis in the evaluation of the strength of mouse femur and tibia. *Bone* 1998; 23:155-161.
  22. Cody DD, Gross GJ, Hou FJ, Spencer J, Goldstein SA, Fyhrie DP. Femoral strength is better predicted by finite element models than QCT and DXA. *J Biomech* 1999; 32:1013-1020.
  23. Strømsøe K, Høiseth A, Alho A, Kok WL. Bending strength of the femur in relation to non-invasive bone mineral assessment. *J Biomech* 1995; 28:857-861.